

## The Temperature Dependence of the Anharmonic Properties of Crystalline Naphthalene- $d_8$

BY E. BAHARIE\* AND G. S. PAWLEY†

*Department of Physics, University of Edinburgh, King's Buildings, Mayfield Road, Edinburgh EH9 3JZ, Scotland*

(Received 24 March 1982; accepted 20 May 1982)

### Abstract

The temperature variation of the unit cell and molecular orientation in perdeuteronaphthalene is measured with considerable accuracy by neutron diffraction from a powder sample in the temperature range from 5 to 293 K. Measurements were done on the D1A and D1B instruments at ILL Grenoble. Results were obtained through constrained refinements using the program *EDINP*. The fundamental problem of background scattering is scrutinized, concluding that even with such a problem it is possible to obtain good measurements of rigid-body thermal-motion tensors by this technique. These results are of importance for the lattice dynamical studies of this system.

### Introduction

Molecular systems as typified by naphthalene and anthracene show pronounced anharmonic effects due to the balance between the weak intermolecular attraction and the strong overlap repulsion. Our understanding of intermolecular forces in the solid state can be considerably enhanced by having extensive measurements of those properties which show a pronounced temperature variation. A number of these properties can be found by crystallographic techniques, and the present work is a study of those properties which are best investigated through neutron diffraction from powder samples. We choose to study naphthalene- $d_8$  as this system has been extensively studied by a number of other techniques, especially in the field of lattice dynamics (Pawley, 1967; Mackenzie, Pawley & Dietrich, 1977; Natkaniec *et al.*, 1980; Schmelzer *et al.*, 1981), for which measurements of the unit cell and molecular orientation are very important.

In the course of this work we feel obliged to go into some detail as regards certain problems inherent in the particular technique used, concluding that certain

quantities can readily be measured accurately by this technique whereas other quantities require a considerable enhancement of the general method before they can be determined with sufficient confidence.

The most obvious anharmonic effect displayed by crystals is the change in unit cell as a function of temperature. The most accurate method of monitoring this change is through the use of diffraction from a powder specimen. Accuracy depends on the calibration of the radiation wavelength used and of the instrument, and in the present work the error due to these two sources is less than that caused by the uncertainty of the absolute temperature. Intimately related to the unit-cell variation is the variation of the molecular orientation within the unit cell. Monitoring this requires a structure refinement, and this immediately introduces more sources of error, both statistical and systematic.

The variation of thermal vibration amplitudes with temperature is only secondarily an anharmonic effect and to be able to observe such an effect we need to investigate whether such amplitudes can be accurately determined by the powder technique. From the powder diffraction work on  $\alpha$ -resorcinol by Bacon, Lisher & Pawley (1979) it would appear that the thermal amplitudes as expressed through the mean-square translational and librational tensors (**T** and **L**) and estimated by structure refinement bear a close relationship to those obtained by a single-crystal analysis. If this is a general result of sufficient accuracy we should be able to search for any anomalous changes in **T** and **L** which might be brought on by the approach to a phase transition. From the early work of Bridgman (1936) a phase change in naphthalene has been suspected to take place at elevated pressure and temperature, and therefore a study of the variation of **T** and **L** with temperature is of value.

The technique of neutron powder diffraction was used on a sample of perdeuteronaphthalene, kindly supplied by Dr Sheka and being of the same batch as that used for the extensive measurements of the phonon dispersion curves (Natkaniec *et al.*, 1980; Schmelzer *et al.*, 1981). A number of scans have been made using the high-resolution diffractometer D1A at the Institut

\* Now at Marconi Space and Defence Systems Ltd, The Grove, Warren Lane, Stanmore, Middlesex HA7 4LY, England.

† Please address correspondence to this author.

Laue–Langevin, Grenoble, but these have been augmented by scans on the multicounter diffractometer D1B. The latter scans are of lower resolution and involve a smaller range of  $\sin \theta/\lambda$ , but nevertheless give independent results which assist in the validation of the resulting structure parameters.

The profile refinement technique (Rietveld, 1969) has been used throughout. Because the unit cell of naphthalene contains many atoms the number of parameters required to refine all atomic positions and thermal parameters independently is too great to give a successful result as the information content of a powder diffraction scan is far less than that of a single-crystal analysis. To overcome this problem extensive constraints are placed on the analysis through the use of the program *EDINP* (Pawley, 1980). As one of the main aims of the work is to measure the tensors **T** and **L** a constraint on the thermal parameters is essential – the unsound technique of determining anisotropic temperature factors independently and then analysing for **T** and **L** would probably fail with a powder diffraction refinement. Furthermore, as it is thought impossible to find small molecular distortions because of the restricted information content of the data, the molecule was assumed to obey *mmm* symmetry throughout, taking the molecule as that determined by Pawley & Yeats (1969). Thus the atomic positions are governed simply by the three Euler angles  $\varphi \theta \psi$ . The implicit assumption in this constraint is that the molecular geometry and size do not change between 5 K and room temperature. This is given considerable support by a recent low-temperature study of anthracene- $d_{10}$  (Chaplot, Lehner & Pawley, 1982) where no significant change in the symmetry-constrained molecule was observed on comparison with the room-temperature result of Lehmann & Pawley (1972), although the data contained sufficient information for significant molecular distortions to be observed through an unconstrained refinement.

### Experimental and refinement

The sample of highly zone-refined naphthalene- $d_8$  was crushed to a fine powder and packed into a vanadium cylinder 16 mm diameter. This was set in a helium cryostat and the first measurements were taken at 5 K. The scan time was 16 h, this length of time being used to increase the chance of success in determining the thermal parameters. The sample was then warmed to 50 K, and was equilibrated for about one hour before an 8 h scan was made. Further 16 h scans were made at 100, 200 and 293 K, these temperatures being controlled to about  $\pm 0.1$  K, the absolute temperature accuracy being roughly  $\pm 3$  K. Data from the array of ten  $^3\text{He}$  counters were combined to give the observed scans shown in Fig. 1, using neutrons of wavelength 1.9090 (1) Å calibrated against a standard nickel sample.

A number of refinements were done on all these scans but we choose to report four models with the following parameter sets.

Models I, II, III, IV	overall scale factor peak shape; $u, v, w$ (see Rietveld, 1969) unit cell; $a, b, c, \beta$ Euler angles; $\varphi \theta \psi$ .
Model I	overall temperature factor; $B$ .
Model II	two isotropic temperature factors, one for C atoms and one for D atoms.
Models III, IV	anisotropic temperature factors determined by <b>T</b> and <b>L</b> plus an extra isotropic temperature factor for D.
Models I, II, III	flat variable background refined.
Model IV	arbitrary background subtracted (see next section).

The weighting scheme used in all refinements is of unit weights for all points in the scan, including the regions where no clear peaks are observable. We choose not to use a weighting scheme based on counting statistics as we consider such random aspects as being the least significant source of error and because such a treatment gives undue emphasis to the fitting of the regions where there is only background scattering. The *R* factors for these refinements are given in Table 1, where

$$R(\%) = 100 \sum |I^{\text{obs}} - I^{\text{calc}}| / \sum I^{\text{obs}}$$

Here the summations are over all points in the scans, and the same denominator is used for model IV as for the other models. The scans all range from  $2\theta = 6$  to  $160^\circ$  in steps of  $0.05^\circ$ , though the refinements use steps of  $0.1^\circ$ , there being no apparent loss of information in averaging adjacent pairs of measurements. The five scans are presented in Fig. 1,\* where

\* The numbered intensity of each measured point on the profile, as a function of scattering angle, has been deposited with the British Library Lending Division as Supplementary Publication No. SUP 36962 (17 pp.). Copies may be obtained through The Executive Secretary, International Union of Crystallography, 5 Abbey Square, Chester CH1 2HU, England.

Table 1. *The R factors (%) for the four models*

Although model IV has an arbitrary background function subtracted, the *R* factor has been calculated using the same denominator as for the others.

Model	5 K	50 K	100 K	200 K	293 K	Parameters
I	6.3	6.7	7.8	10.4	11.2	14
II	5.7	5.9	6.8	9.2	10.2	14
III	5.0	5.1	5.9	8.3	8.5	27
IV	4.9	4.9	4.5	3.8	4.4	26*

\* Indicates that some parameters should be added because of the arbitrary background function.

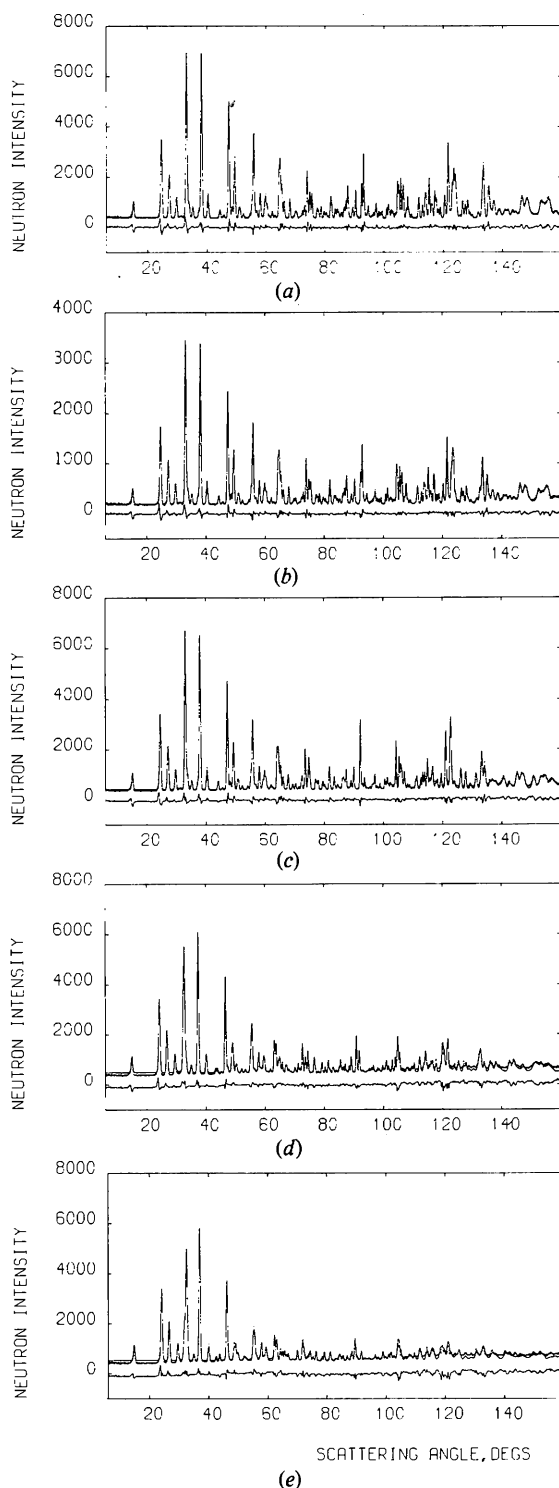


Fig. 1. The intensity in the observed and calculated diffraction scans from  $2\theta = 6$  to  $160^\circ$  in steps of  $0.1^\circ$ , neutron wavelength =  $1.9090$  ( $1$ )  $\text{\AA}$ , for temperatures (a) 5 K, (b) 50 K, (c) 100 K, (d) 200 K, (e) 293 K. The calculated background in each case was a refined value, constant with  $2\theta$ , clearly showing inadequacy at the scan extremes. The difference intensity, observed-calculated, is plotted beneath each scan, where the calculated scan corresponds to model III.

the calculated scan involves a flat background in each case.

The intricacies of profile refinement are such that no satisfactory statistical foundation has as yet been developed for powder diffraction refinements and we therefore feel unable to perform a thorough  $F$ -distribution test. Table 1 must therefore be evaluated subjectively. Model IV appears to approach the best possible fit for each scan, and is marginally better than model III at the low temperatures. Models I, II and III all show the worsening of the fit as temperature is increased, clearly showing the growing inadequacy of the refinable flat background. However, it is clear that at all temperatures model III is better than model II, which in turn is better than model I. The differences between models I and II at all temperatures show that the extra parameter introduced by allowing C and D atoms to have independent isotropic temperature factors is valid. Similarly the improvement gained by introducing T and L (model III) would seem to be highly significant as there is a clear pattern to the improvement as a function of temperature, this being more pronounced at the higher temperatures.

Those parameters which were common to the various models differed so little in value between the models that inclusion of separate entries in Tables 2 and 3 would be meaningless. Table 2 gives the values for the scan parameters, and as there was an indication that these parameters were better determined by models III and IV, the average of the results from these models is given. The parameter showing the biggest discrepancy between models III and IV is the scan zero, and this discrepancy is only larger than its least-squares standard deviation for the runs at 200 and 293 K. In these cases it would appear that a better estimate for the standard deviation than that given would be  $\sigma \sim 0.02^\circ$ .

#### The background function

One aspect of profile refinement which has not been given sufficient attention by workers in the field is that concerning the background function. The customary procedure followed in most studies is to subtract an arbitrary background from the scan and then to discard those regions where no obvious diffraction peaks occur. The adjective 'arbitrary' is used here as the subtracted function is not based on the physics of the system under consideration but is determined subjectively by choosing a line which best fits the background in those regions devoid of diffraction peaks. The scans of Fig. 1 show that this procedure becomes very difficult at high diffraction angles, and we will see that this leads to inaccuracies in all the thermal parameters.

At very low temperatures the main contribution to the background scattering comes from incoherent scattering which, for a well-adjusted instrument, should be well represented by a flat background. This is

Table 2. *The scan parameters; overall scale, background count (not IV), scan zero and u, v, w*

The averages for models III and IV are taken here; they differ by more than the quoted standard deviations only for 200 and 293 K data.

		5 K	50 K	100 K	200 K	293 K
Overall scale factor		0.778 (3)	0.386 (1)*	0.759 (3)	0.738 (4)	0.705 (5)
Flat background		376 (2)	194 (1)	425 (2)	495 (3)	531 (3)
Scan zero of $2\theta$ (°)		0.262 (1)	0.263 (1)	0.268 (2)	0.280 (3)	0.286 (4)
Peak shape parameters	$u$	0.207 (4)	0.209 (4)	0.221 (5)	0.283 (14)	0.488 (35)
	$v$	-0.526 (9)	-0.521 (10)	-0.530 (11)	-0.577 (26)	-0.661 (53)
	$w$	0.451 (4)	0.446 (4)	0.443 (5)	0.445 (9)	0.459 (15)

\* This run was done with 50% statistics.

Table 3. *The well-determined structural parameters; unit-cell constants, and volume, Eulerian angles*

The values are averages of models III and IV. An argument is given in the text that the Euler angle standard errors should be increased by a factor of five to attempt to allow for systematic errors.

	5 K	50 K	100 K	200 K	293 K
$a$ (Å)	8.0711 (1)	8.0798 (2)	8.1048 (2)	8.1701 (2)	8.2306 (4)
$b$ (Å)	5.9272 (1)	5.9303 (1)	5.9385 (1)	5.9582 (2)	5.9760 (3)
$c$ (Å)	8.6240 (1)	8.6288 (1)	8.6388 (1)	8.6575 (2)	8.6667 (5)
$\beta$ (°)	124.661 (1)	124.582 (1)	124.369 (2)	123.738 (2)	122.984 (4)
$V$ (Å <sup>3</sup> )	339.35 (1)	340.40 (2)	343.20 (2)	350.46 (2)	357.58 (4)
$\nu$ (°)	293.73 (3)	293.69 (3)	293.57 (4)	293.30 (7)	292.67 (7)
$\mu$ (°)	248.87 (4)	249.05 (4)	249.33 (4)	250.37 (6)	251.52 (4)
$\omega$ (°)	116.87 (5)	116.89 (5)	116.88 (6)	117.22 (8)	117.97 (6)

supported by the very small difference between the refined models III and IV at 5 K. At higher temperatures the thermal diffuse scattering increases, and as this is a function of scattering angle the flat background function becomes progressively poorer. To date no satisfactory background function has been used in profile refinements to take account of this thermal scattering, although Windsor & Sinclair (1976) have suggested the use of a smoothly increasing background determined by the overall temperature factor. This suggestion stems from the fact that the scattering intensity lost from Bragg peaks appears as background. In the present case this result seems to be well founded, as the total scattering in the five scans is remarkably constant, the figures being 5 K 1 167 876 counts, 50 K 1 160 814 counts (as for a long run), 100 K 1 163 786 counts, 200 K 1 161 824 counts, 300 K 1 171 722 counts. For the 293 K scan about half the total count lies below a flat background (370 counts), one quarter is background above this value and the last quarter is in the Bragg intensities. The disadvantage of the Windsor-Sinclair suggestion is seen in Fig. 2. Here the subtracted background functions are plotted together, and it is clear that the variation is not a smooth monotonically increasing function. This figure shows furthermore the subjectivity involved in choosing the function as the choice of 293 K is clearly inconsistent with those at lower temperatures especially in the regions of high scattering angles. We see in the next section that this inconsistency gives rise to unreliability in the thermal parameters.

Another possible source of error in the thermal parameters stems from the neglect of an absorption correction, but this is thought not to be serious in the present case as the flat background function appears to be quite appropriate for the 5 K data.

#### Temperature parameters (Table 4)

The purpose behind giving the D atoms an extra isotropic temperature factor  $\bar{u}_d^{2+}$  is to allow for the extra D motion caused by the internal modes. The thermal increase of  $\bar{u}_d^{2+}$  in model II is too great to be caused only by the internal motion, and is clearly due to the temperature increase of the librational amplitudes as librational motion moves the peripheral D atoms preferentially. In models III and IV, however, where the librational motion is specifically accounted for, an increase in  $\bar{u}_d^{2+}$  is not statistically significant – this is physically reasonable as it corresponds to a motion which is not classical even at the higher temperatures, a motion associated with a frequency somewhat in excess of 6 THz ( $\equiv kT$  at  $T \sim 300$  K).

The T tensor\* as given by model III does not behave physically at higher temperatures, at which negative

\* T and L are expressed throughout with respect to orthogonal axes along **a**, **b** and **c**.\*

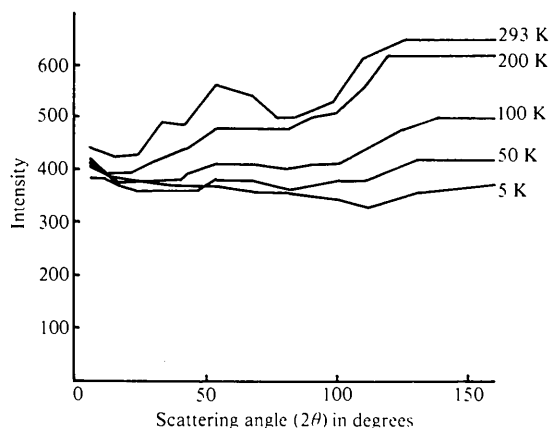


Fig. 2. The arbitrary background functions subtracted from the scans at the five different temperatures, for model IV.

Table 4. *Temperature parameters for the four models*

The units are  $\text{\AA}^2 \times 10^{-2}$  for the mean-square displacements and **T** tensor coefficients, degrees squared for the **L** tensor coefficients. The superscript + on the mean-square displacements for models III and IV indicates that this is an extra thermal effect, over and above the rigid-body motion. The errors quoted refer to the last figure of the preceding value, and show a clear increase with temperature.

	5 K	50 K	100 K	200 K	293 K
I $\bar{u}^2$	1.26 (2)	1.42 (3)	1.87 (3)	2.91 (6)	3.41 (9)
II $\bar{u}_c^2$	0.85 (5)	0.91 (6)	1.12 (7)	1.74 (14)	1.86 (24)
$\bar{u}_d^2$	1.79 (5)	2.08 (6)	2.94 (7)	4.96 (14)	6.90 (24)
III $\bar{u}_d^{2+}$	0.66 (9)	0.67 (9)	0.85 (11)	1.00 (22)	0.52 (29)
$T_{11}$	0.48 (14)	0.25 (14)	0.08 (15)	0.03 (28)	0.11 (44)
$T_{22}$	0.34 (8)	0.17 (7)	-0.18 (8)	0.07 (15)	-0.31 (20)
$T_{33}$	1.19 (7)	1.26 (7)	1.27 (8)	1.73 (16)	0.64 (22)
$T_{23}$	-0.16 (5)	-0.08 (6)	0.07 (6)	-0.42 (15)	-0.96 (19)
$T_{31}$	-0.17 (8)	-0.21 (8)	-0.34 (8)	-0.51 (18)	-0.79 (25)
$T_{12}$	-0.06 (8)	0.07 (8)	0.18 (8)	0.01 (17)	0.07 (28)
$L_{11}$	4.3 (10)	7.0 (10)	15.5 (12)	27.2 (24)	53.5 (36)
$L_{22}$	2.8 (9)	4.2 (9)	5.9 (10)	14.4 (20)	20.2 (31)
$L_{33}$	4.6 (16)	7.5 (16)	13.6 (19)	20.5 (37)	33.6 (57)
$L_{23}$	0.6 (5)	-0.1 (6)	-0.6 (7)	-3.0 (14)	-5.3 (19)
$L_{31}$	-2.4 (9)	-3.4 (10)	-4.9 (11)	-5.4 (24)	-11.8 (36)
$L_{12}$	0.4 (5)	0.7 (5)	1.8 (6)	1.3 (13)	0.3 (23)
IV $\bar{u}_d^{2+}$	0.93 (9)	0.81 (10)	1.08 (10)	0.99 (14)	1.10 (21)
$T_{11}$	0.52 (14)	0.73 (14)	1.02 (15)	1.79 (20)	1.89 (30)
$T_{22}$	0.24 (7)	0.41 (8)	0.58 (8)	1.78 (11)	1.58 (15)
$T_{33}$	1.05 (7)	1.41 (7)	1.76 (8)	3.40 (11)	3.61 (17)
$T_{23}$	-0.14 (5)	-0.05 (6)	0.05 (6)	0.01 (10)	-0.52 (13)
$T_{31}$	-0.08 (7)	-0.11 (8)	-0.16 (8)	-0.47 (13)	-0.56 (18)
$T_{12}$	-0.12 (7)	0.00 (8)	-0.00 (8)	0.17 (12)	0.07 (19)
$L_{11}$	2.8 (9)	5.5 (10)	9.4 (11)	17.4 (15)	30.3 (22)
$L_{22}$	1.8 (9)	2.5 (9)	4.5 (9)	11.0 (13)	18.4 (20)
$L_{33}$	2.0 (15)	3.7 (16)	4.8 (17)	12.6 (23)	22.0 (36)
$L_{23}$	0.7 (5)	0.0 (5)	-0.9 (6)	-2.3 (8)	-4.1 (11)
$L_{31}$	-1.2 (9)	-2.7 (9)	-2.2 (10)	-5.4 (15)	-6.1 (23)
$L_{12}$	0.2 (5)	0.5 (5)	1.5 (6)	3.6 (8)	1.7 (14)

diagonal elements appear. Such behaviour does not occur with model IV, showing the fundamental importance of a background correction. In model IV the diagonal elements at 293 K are 1.89, 1.58 and  $3.61 \text{\AA}^2 \times 10^{-2}$  which can be compared with 4.84, 2.92 and  $2.29 \text{\AA}^2 \times 10^{-2}$  as determined by Pawley & Yeats (1969) with a single-crystal analysis. The elements of the **T** tensor are thus not very well determined by powder diffraction. Improvements in the estimation of **T** will result when a reliable background function is developed. The inadequacies of the function used depend only on the Bragg scattering angle and are expected therefore to affect the isotropic temperature factors the most, the **T** values less and the **L** values least.

The comparison of the diagonal **L** tensor components at room temperature is much more satisfactory. Here we find 30.3, 18.4 and  $22.0 (^\circ)^2$  as compared with 31.6, 18.5 and  $19.1 (^\circ)^2$  found by Pawley & Yeats (1969). This comparison is indeed excellent, and means that librational motion can be studied in detail by the powder technique. Nevertheless one must be cautious — experience shows that there is considerable

correlation between the components of **L** and those of **T**, especially between the diagonal elements. Thus a reliable estimate of **L** depends in some measure on our ability to determine the true background function.

#### *Reliability of results*

As a test of the reliability of the results just presented, the same sample was used with a completely different powder diffraction instrument, D1B. This instrument contains an array of counters positioned on an arc of a circle, at  $0.2^\circ$  intervals. For the experiments here analysed the counters covered the range  $2\theta = 12$  to  $92^\circ$  with a neutron wavelength  $\lambda = 2.522 (1) \text{\AA}$ . Thus the control experiment has a maximum value of  $\sin \theta/\lambda$  of  $0.29 \text{\AA}^{-1}$  as compared with  $0.52 \text{\AA}^{-1}$  on D1A. Scans were taken at 5, 50 and 100 K, an arbitrary background was subtracted and the model II refinements then reached *R* factors of 6.1, 6.9 and 6.9% respectively.

No attempt was made to refine **T** and **L**, owing to the low resolution of the data (restricted  $\sin \theta/\lambda$  range). The final results of the unit cell and Eulerian angles are

given in Table 5, which can be compared directly with Table 3. The unit cells are much better determined by the high-resolution scans, the unit-cell edges agreeing to within the estimated standard deviations whereas the interaxial angles  $\beta$  differ by at most  $3\sigma$ (D1B). The tabulated results yield an estimate for the thermal expansion, and it can be seen that the standard deviations quoted for the unit-cell edges are comparable with the changes produced by 1 K, and therefore the measurement of the absolute temperature limits the accuracy of the final result.

The discrepancies between the D1A and D1B results for the Eulerian angles, however, are considerably greater than for the cell constants, reaching about  $20\sigma$ (D1B) for some  $\theta$  values; this suggests that the least-squares standard deviations calculated for these structural parameters are too small. It has been suggested by Pawley (1980) that a more realistic standard error can be found for *structure* parameters by using a modified value for the number of points in the scan,  $N$ . The standard errors given by the least-squares procedure contain the factor  $N^{-1/2}$ , suggesting that any desired accuracy can be achieved simply by taking small enough scan steps. The fallacy in this argument has been explained by Sakata & Cooper (1979), and to overcome the problem we examine the simple expedient of replacing  $N$  by  $N/n$ , where  $n$  is the number of scan points corresponding to an average full width of a single peak at half height. Adopting this procedure leads to standard errors for the D1A scans increased by a factor of five, and for D1B scans by a factor of four. Thus, for example, we would get for the 5 K results:

	$\varphi$	$\theta$	$\psi$
D1A	293.7 (2)°	248.9 (2)°	116.9 (3)°
D1B	293.9 (3)	249.9 (2)	118.0 (3)

The closer consistency of these results suggests that the standard errors are more realistic.

Finally, a comparison can be made between the Eulerian angles at room temperature obtained from this

Table 5. *The well-determined structural parameters resulting from the lower-resolution D1B scans*

These values are to be compared with those of Table 3, the D1A scan values.

	5 K	50 K	100 K
$a$ (Å)	8.0714 (4)	8.0797 (5)	8.1061 (5)
$b$ (Å)	5.9275 (6)	5.9318 (6)	5.9391 (7)
$c$ (Å)	8.6238 (5)	8.6278 (5)	8.6382 (6)
$\beta$ (°)	124.670 (3)	124.593 (4)	124.380 (4)
$V$ (Å <sup>3</sup> )	339.33 (7)	340.40 (8)	343.22 (9)
$\varphi$ (°)	293.94 (7)	293.82 (7)	293.57 (8)
$\theta$ (°)	249.92 (5)	250.10 (6)	250.29 (5)
$\psi$ (°)	118.03 (7)	118.08 (7)	117.98 (7)

work and from single-crystal work (Pawley & Yeats, 1969). The latter values are

$$\varphi, \theta, \psi = 292.92 (5), 251.79 (6), 117.98 (7)^\circ,$$

which agree with the present results within the newly suggested standard deviations.

## Discussion

The temperature effects on naphthalene- $h_8$  have recently been investigated by Brock & Dunitz (1982) (BD), using X-ray techniques. It is unfortunate that the deuterated material, for which we have a chance of a complete study, is not the natural material as the latter has always been chosen for X-ray study. Thus the comparison of our results with those of BD involves the extra complication of deuteration effects. One would assume that the intermolecular forces would be independent of isotopic composition, the deuterated material behaving in many ways like the hydrogenated material at a lower temperature. This is seen in Fig. 3, where the present results are compared with the results of BD and of Ryzhenkov & Kozhin (1968) (RK). The  $C_{10}D_8$  cell-edge constants are systematically slightly smaller than those for  $C_{10}H_8$  of BD, though the results of RK show a more erratic behaviour. These cell constants are the most accurate results to come from the present work, and comparison with BD shows that the  $C_{10}D_8$  unit-cell volume is 0.3, 0.4 and 1.3% smaller than the  $C_{10}H_8$  cell at 100, 200 and 300 K respectively.

Associated with this unit-cell behaviour one would expect the rigid-body thermal-motion tensors  $\mathbf{T}$  and  $\mathbf{L}$

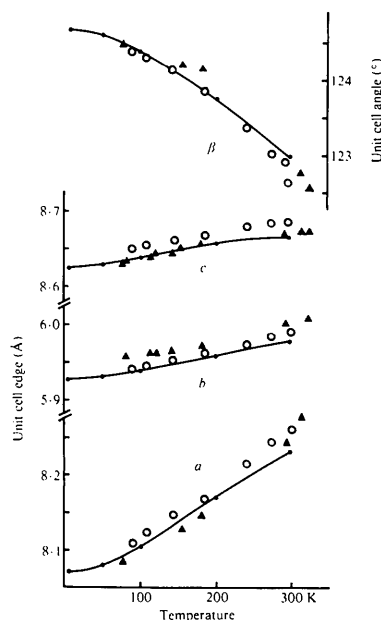


Fig. 3. Comparison of the unit-cell constants for  $C_{10}D_8$  of this work (filled circles joined by guide lines) and for  $C_{10}H_8$  of Brock & Dunitz (1982), (open circles), and of Ryzhenkov & Kozhin (1968), (filled triangles).

to be greater for  $C_{10}H_8$  than for  $C_{10}D_8$ . These are compared with BD in Fig. 4, where their results come from their Fig. 7. The results are not fully comparable as BD in this figure present  $T_{ii}$  and  $L_{ii}$  uncorrected for internal motion, whereas the values from Table 4 are from refinements where the principal internal-mode contribution is in part included through the use of an extra isotropic temperature parameter for D's. Nevertheless, BD show how the internal motion affects  $T_{ii}$  and  $L_{ii}$ , and the changes are small compared with the differences with the present results for  $L_{ii}$ . Fig. 4 shows that the present results for  $T_{ii}$  do agree in the range given by BD better than would be expected from the aberrant behaviour of the 293 K result. It would have been most useful if BD had presented their results at this temperature in their paper.

Comparison of  $L_{ii}$  is the most remarkable, with  $L_{11}(C_{10}D_8)$  consistently much larger than  $L_{11}(C_{10}H_8)$ . In this case (except for deuteration) the single-crystal results of Pawley & Yeats (1969) (PY) are directly comparable with uncorrected BD. At 295 K the PY measurements are in very good agreement with model IV in Table 4. The PY result does not involve a correction for internal motion, whereas a partial correction is achieved in the present powder diffraction result as argued above. However, BD shows that the effect of correcting for internal motion on the X-ray result is to *increase* rather than decrease the values of  $L_{ii}$ . Such behaviour may be a result of the fact that X-ray studies can never yield anisotropic temperature factors for hydrogen atoms of sufficient accuracy for

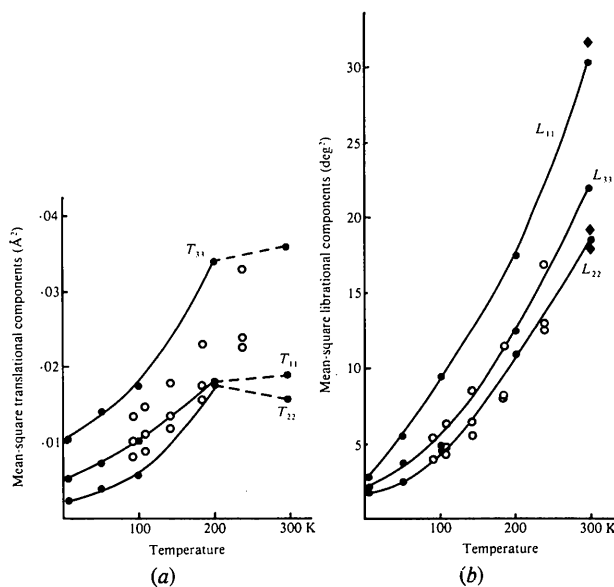


Fig. 4. The diagonal components of the (a)  $T$  tensor and (b)  $L$  tensor as a function of temperature for  $C_{10}D_8$  (filled circles and guide lines) and for  $C_{10}H_8$  after BD (open circles). The upper entries correspond (a) to  $T_{33}$  and (b) to  $L_{11}$  for each temperature. The coordinate system is related to the crystal axes in the order  $a$ ,  $b$ ,  $c^*$ . The filled diamonds are from PY.

this type of analysis, and therefore give results based entirely on the molecular-framework atoms. A full correction for internal motion may well reduce the  $L$  values in the case of results from neutron scattering experiments where the deuterium scattering is of major importance.

A final comparison for librational motion is given in Fig. 5, where each result presented is the trace of  $L$  ( $= L_{11} + L_{22} + L_{33}$ ). The present results give the largest values, showing agreement with PY, being systematically 10% larger than BD. The uncorrected BD result is consistent with that of Cruickshank (1957), which is very close to the lattice dynamical calculation of Pawley (1967). A correction of Cruickshank's result would leave it still close to the lattice dynamical result. The result of Ponomarev, Filipenko & Atovmyan (1976) at 125 K is surely too small? The overall consistency of all these results leads us to conclude that our results from powder neutron diffraction give a very good measure of the librational motion of sufficient quality that internal-motion correction would be justifiable. A similar statement for the  $T$  tensor may be possible when a valid background correction is developed.

The present work has shown that the powder diffraction neutron scattering technique gives a clear picture of fundamental anharmonic temperature effects – the variation of unit cell and molecular orientation. For such results the D1B scans would seem to be adequate. On the other hand, the higher quality D1A scans do give a better estimate of these parameters and the possibility of monitoring the rigid-body motions of the molecules with some precision.

We wish to thank Dr E. F. Sheka for the sample material and Dr J. S. W. Overell for help with some of the figures. One of us (EB) was supported by the

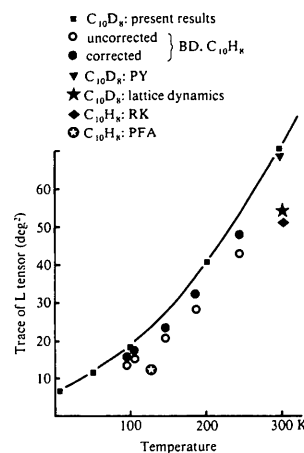


Fig. 5. The trace of  $L$  ( $= L_{11} + L_{22} + L_{33}$ ) as a function of temperature for  $C_{10}D_8$  and  $C_{10}H_8$ , obtained both experimentally and theoretically.

Science and Engineering Research Council (UK) for which we are grateful. Furthermore, we thank Professor Jack Dunitz for sending us his work in preprint form, and Dr Alan Hewat for many helpful suggestions during the writing of this paper, after giving considerable help with the experiment at the Institut Laue-Langevin, Grenoble.

#### References

- BACON, G. E., LISHER, E. J. & PAWLEY, G. S. (1979). *Acta Cryst.* B35, 1400–1403.  
 BRIDGMAN, P. W. (1936). *Proc. Am. Acad. Arts Sci.* 72, 227–266.  
 BROCK, C. P. & DUNITZ, J. D. (1982). *Acta Cryst.* B38, 2218–2228.  
 CHAPLOT, S. L., LEHNER, N. & PAWLEY, G. S. (1982). *Acta Cryst.* B38, 483–487.  
 CRUICKSHANK, D. W. J. (1957). *Acta Cryst.* 10, 504–508.  
 LEHMANN, M. S. & PAWLEY, G. S. (1972). *Acta Chem. Scand.* 26, 1996–2004.  
 MACKENZIE, G. A., PAWLEY, G. S. & DIETRICH, O. W. (1977). *J. Phys. C.* 10, 3723–3736.  
 NATKANIEC, I., BOKHENKOV, E. L., DORNER, B., KALUS, J., MACKENZIE, G. A., PAWLEY, G. S., SCHMELZER, U. & SHEKA, E. F. (1980). *J. Phys. C.* 13, 4265–4283.  
 PAWLEY, G. S. (1967). *Phys. Status Solidi*, 20, 347–360.  
 PAWLEY, G. S. (1980). *J. Appl. Cryst.* 13, 630–633.  
 PAWLEY, G. S. & YEATS, E. A. (1969). *Acta Cryst.* B25, 2009–2013.  
 PONOMAREV, V. I., FILIPENKO, O. S. & ATOVMIAN, L. O. (1976). *Sov. Phys. Crystallogr.* 21, 215–216.  
 RIETVELD, H. M. (1969). *J. Appl. Cryst.* 2, 65–71.  
 RYZHENKOV, A. P. & KOZHIN, V. M. (1968). *Sov. Phys. Crystallogr.* 12, 943–945.  
 SAKATA, M. & COOPER, M. J. (1979). *J. Appl. Cryst.* 12, 554–563.  
 SCHMELZER, U., BOKHENKOV, E. L., DORNER, B., KALUS, J., MACKENZIE, G. A., NATKANIEC, I., PAWLEY, G. S. & SHEKA, E. F. (1981). *J. Phys. C.* 14, 1025–1041.  
 WINDSOR, C. G. & SINCLAIR, R. N. (1976). *Acta Cryst.* A32, 395–409.

*Acta Cryst.* (1982). A38, 810–813

## Observation of Effect of Temperature on X-ray Diffraction Intensities across the In $K$ Absorption Edge of InSb

BY T. FUKAMACHI

*Saitama Institute of Technology, Okabe, Saitama 369-02, Japan*

T. KAWAMURA

*Faculty of Education and Liberal Arts, Yamanashi University, Kofu, Yamanashi 400, Japan*

K. HAYAKAWA

*Central Research Laboratory, Hitachi Ltd, Kokubunji, Tokyo 185, Japan*

AND Y. NAKANO AND F. KOH

*Saitama Institute of Technology, Okabe, Saitama 369-02, Japan*

(Received 5 April 1982; accepted 24 May 1982)

#### Abstract

Variations at room and liquid-nitrogen temperatures have been observed of the energy-dispersive integrated X-ray reflection intensity from an InSb single crystal across the In  $K$  absorption edge by the use of a multi-channel solid-state detector. The results show that the relative intensities from a nearly perfect crystal change as a function of the temperature above and below the absorption edge, but there is no such change in a nearly mosaic crystal. This variation observed in a

nearly perfect crystal is characteristic of an absorbing monatomic perfect crystal and can be explained in terms of the dynamical theory of diffraction including anomalous scattering.

#### Introduction

Across the absorption edge, the integrated X-ray reflection intensity  $J(\omega)$  shows a characteristic variation as a function of X-ray energy  $\hbar\omega$ , depending on